Conformational switching of CD81 controls its function as a receptor for hepatitis C virus

Machaela Palor[1,a], **Lenka Stejskal**[1,2,a], **Piya Mandal**[1], **Adrian J. Shepherd**[2], **and Joe Grove**[1,✉]

[1]Institute of Immunity and Transplantation, Division of Infection and Immunity, The Royal Free Hospital, University College London, NW3 2PF
[2]Institute of Structural and Molecular Biology, Birkbeck College, University of London, London, United Kingdom
[a]These authors contributed equally to this work

CD81 is a multifunctional protein that plays a central role in both physiological and pathological processes. Recent structural analysis of CD81 indicates that it adopts a compact fold with its large extracellular loop sitting close to the plasma membrane; however, there is evidence that CD81 can undergo a conformational switch where the extracellular loop flips into an extended open conformation. We investigated the relevance of CD81 conformational switching to its function as a receptor for hepatitis C virus (HCV). Structure-led mutagenesis was used to generate CD81 variants with altered conformational switching. Each variant maintained proper protein folding and expression, and retained a basic function: the ability to chaperone CD19 to the cell surface. We then used multiple systems to evaluate HCV receptor activity; in these experiments 'open' CD81 variants exhibited consistently poor receptor function, whereas a 'closed' CD81 displayed enhanced ability to support HCV entry. We sought to corroborate these findings by exploring CD81 structural flexibility using molecular dynamics simulations. These experiments were in excellent agreement with our in vitro work, with 'open' CD81 variants having a propensity to undergo conformational switching. Taken together, we provide evidence for a conformational switch in CD81 that regulates its HCV receptor activity. This work furthers our understanding of the molecular mechanism of HCV entry and is relevant to CD81's other functions in health and disease.

tetraspanin | hepatitis C | virus entry

Correspondence: ***j.grove@ucl.ac.uk***

Introduction

Binding of the E2 glycoprotein of hepatitis C virus (HCV) to the large extracellular loop of CD81 is a defining event in the entry of HCV [1] and is targeted by multiple broadly neutralising antibodies; thus placing this molecular interaction at the forefront of current HCV vaccine development [2,3]. Whilst the importance of CD81 in HCV entry is well established, the precise details of E2-CD81 interaction have yet to be defined and the molecular determinants of CD81 receptor activity are only partially understood [4].

CD81 is a prototypical member of the tetraspanin superfamily. Tetraspanins are small integral membrane proteins, defined by their four transmembrane domains separated by intra/extracellular loops. Highly conserved cysteine residues stabilise tetraspanin tertiary structure through disulphide bridges, and provide sites for post-translational palmitoylation, which influences tetraspanin membrane segregation [5,6].

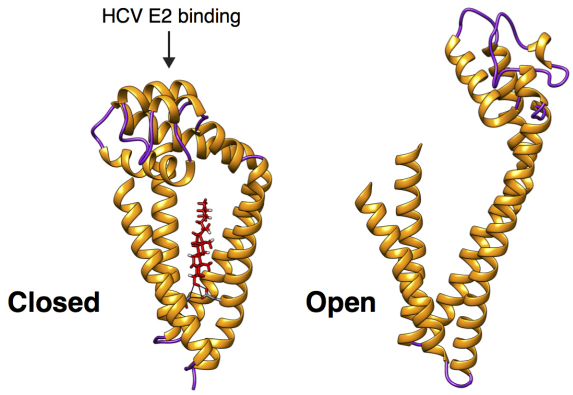

Fig. 1. Conformational switching of CD81 Molecular models of CD81 in the closed and open conformations; the closed conformation is based on the crystal structure (PDB: 5TCX), whereas the open conformation was generated by molecular dynamic simulations, as described by Zimmerman et.al. Alpha helices are shown in gold, whereas unstructured regions are in purple, cholesterol is shown in red. HCV binds to helices D and E of the EC2, as indicated. The small EC1 is unstructured in both the open and closed conformations and has been omitted from the image for clarity.

Largely without cognate ligands, tetraspanins participate indirectly in a wide variety of cell-biological processes through their interactions with partner proteins, which they organise into functional complexes [7,8]. For example, CD81 facilitates the assembly of the B-cell receptor complex and is therefore essential for normal antibody responses. CD81 performs this role via partnership with CD19; first by chaperoning CD19 through the secretory pathway and then by dictating its cell surface distribution, which permits proper assembly of the B-cell receptor complex upon activation [9–12]. Through other molecular partnerships CD81 has been implicated in additional physiological processes such as T-cell receptor signalling, cell migration, growth factor signalling, sperm-egg fusion and most recently, biological ageing [13–18].

Aside from these physiological functions, CD81 is also commandeered by diverse infectious pathogens. It participates in the cell-surface assembly of both human immunodeficiency virus (HIV) and influenza A virus; a function that may be linked to the apparent affinity of CD81 for membrane structures with high curvature [19–22]. CD81 also negatively regulates SAMHD1 function, resulting in increased intracellular pools of dNTPs, which in turn favours HIV reverse transcription [23]. Finally, CD81 is critical for the entry of HCV and *Plasmodium* sporozoites into human hepatocytes

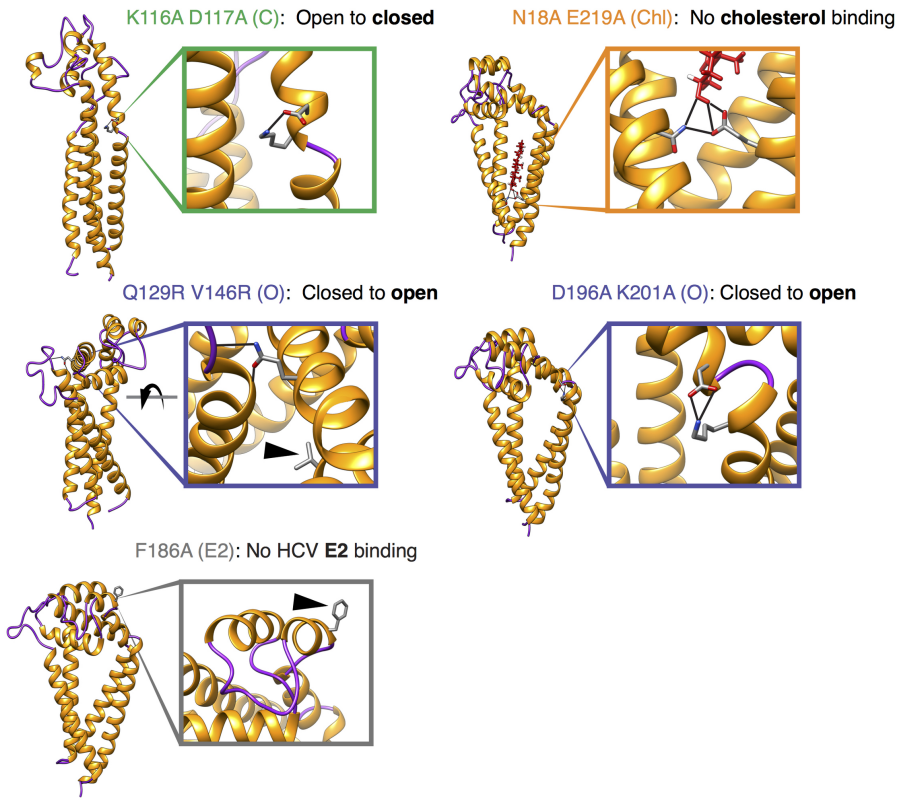

Fig. 2. Structure led mutagenesis We designed mutations that would shift CD81 either towards a closed or open conformation, we also disrupted the ability of CD81 to interact with cholesterol and the E2 glycoprotein of HCV. The images present CD81 structures displaying the molecular features targeted by each mutation. Black lines represent the hydrogen bonds and salt bridges targeted through mutation. Arrowheads indicate other mutated residues. The expected phenotype is displayed in bold. The rationale for each mutation is outlined in the main text.

[1,24]. In summary, CD81 is a multifunctional protein and a greater understanding of its molecular characteristics will provide novel insights into various physiological and pathological processes.

The recent full crystal structure of CD81, the first of any tetraspanin, has provided a novel perspective on its molecular biology [25]. CD81's four helical transmembrane domains are arranged in a loose bundle forming an inverted conical shape. Curiously, the transmembrane domains form a central intramembrane cavity filled by a single molecule of cholesterol, which is coordinated by hydrogen bonding to the side chains of inward-facing amino acids (Fig. 1A). Whilst this observation may have arisen due to the presence of cholesterol in the crystallisation buffer, Zimmerman et. al. use biochemical experiments to demonstrate physical association of CD81 with cholesterol in cells. Moreover, this finding is consistent with other reports linking cholesterol to tetraspanin biology [26,27].

Whereas the minor extracellular domain (EC1) was not resolved in the crystal structure, CD81's major extracellular domain (EC2) was found to be roughly parallel to the plane of the plasma membrane, analogous to a lid sitting on top of the bundle of transmembrane domains (Fig. 1A). Overall, CD81 adopts a compact structure that is likely to project only a few nanometers from the cell surface. However, using molecular dynamics (MD) simulation Zimmerman et. al. demonstrated that the EC2 of CD81 has a propensity to flip up in to an extended open conformation (Fig. 1B). Furthermore, removal of cholesterol from the intramembrane cavity during the simulations increased the frequency of conformational switching. This observation raises the possibility that cholesterol is acting as an allosteric regulator of CD81 conformation, and raises an obvious question: what role might conformational switching play in CD81 function?

Given our research interests, we initially considered how this CD81 structure might be reconciled with the current understanding of HCV entry. Whilst the precise molecular interaction of E2 with the EC2 has yet to be structurally defined, the relevant protein domains have been identified [28–33]. The viral CD81 binding site comprises discontinuous protein sequences, brought together in the 3D structure of the E2 glycoprotein; these interact with helices D and E of CD81's EC2, which are presented at the apex of CD81's closed compact structure (Fig. 1A). Antibodies that prevent this interaction block HCV entry, and cells without CD81 are completely resistant to infection [34–43]. The ability of CD81 to recruit molecular partners is also likely to be important for HCV infection; indeed, other HCV entry factors constitutively associate with CD81 [8,44]. Significantly, HCV entry also seems to be closely-linked to cell-surface cholesterol transport: three cholesterol-transporting proteins (SR-B1, LDLR and NPC1L1) have been implicated in the process [45]. Notably, the cholesterol transporter SR-B1 naturally associates with CD81 and also modulates the CD81-dependent invasion of *Plasmodium* sporozoites into hepatocytes [8,46,47].

We initiated this study with a simple hypothesis: HCV entry is dependent on the closed conformation of CD81. As intimated in the previous paragraph, there are two pieces of evidence that led us to this notion. First, in the closed confor-

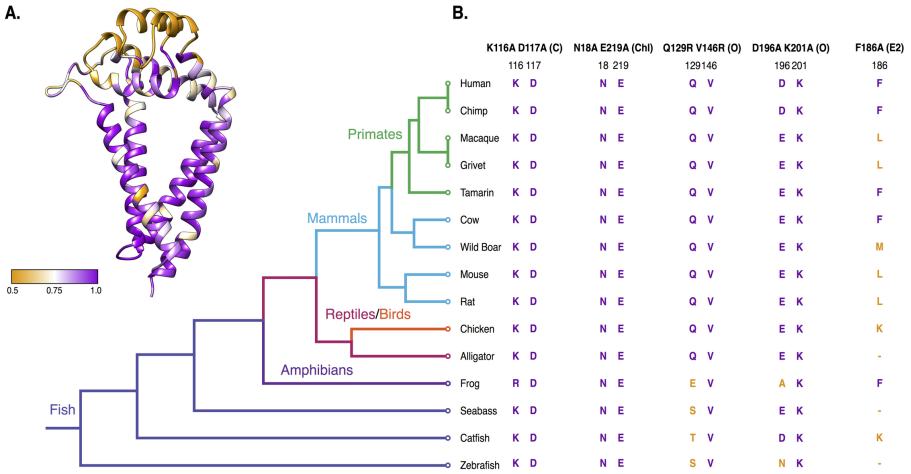

Fig. 3. Evolutionary conservation of CD81 A. CD81 model (based on the crystal structure) with each residue colour-coded for conservation, purple indicates high conservation whilst gold represents low conservation (<0.5), as annotated. The conservation score was generated from an alignment containing 228 vertebrate CD81 genes. **B.** A phylogenetic tree containing representative vertebrate species; the amino acid identity at each site targeted by mutation is annotated. The letters are colour-coded, similar to A., to indicate conservation or divergence, relative to the sequence of human CD81.

mation the E2 binding residues of CD81 are outwardly presented at the apex of the molecule (Fig. 1); we reasoned that this would favour engagement with an incoming virus particle. Second, the high cholesterol dependence of HCV entry [48–50] may suggest that the virus favours the cholesterol bound (i.e. closed) form of CD81.

To investigate this we used structure-led mutagenesis to tip the dynamic equilibrium of CD81 towards either an open or closed conformation. We assessed mutant protein expression and basic function to demonstrate normal folding and availability at the cell surface. We then used various systems to evaluate the HCV receptor activity of each CD81 variant; these experiments were consistent with our hypothesis. Finally, in lieu of a direct assay of CD81 conformation, we evaluated our CD81 variants by MD simulations; the CD81 variants behaved as expected and in excellent agreement with our functional assays. In conclusion, this study suggests that conformational switching of CD81 is a functionally important event that has a direct impact on HCV entry.

Results

Structure-led mutagenesis. We drew upon specific features of the open and closed structures of CD81 [25] to design a panel of amino acid substitutions that we expected to alter conformation. Note, that due to the dynamic nature of conformational switching it can be assumed that a cell will possess a mixture of open and closed molecules within its entire population of CD81. Moreover, it is probable that the specific mutations shift this dynamic equilibrium such that more/fewer molecules are in either state.

The substitutions and their targeted molecular features are outlined in Figure 2. To achieve a predominantly closed conformation we disrupted a salt bridge that appears to stabilise the open form of CD81 (K116A D117A). To prevent cholesterol binding we mutated the inward-facing residues in transmembrane domains (TMD) 1 and 4 that coordinate cholesterol (N18A E219A); substitutions at these sites have previously been demonstrated to prevent CD81 association with cholesterol [25]. Given the findings of Zimmerman et. al. we may expect this mutant to exhibit a predominantly open conformation, albeit via an indirect allosteric mechanism. We generated two mutants that directly favour the open conformation. In Q129R V146R we prevented hydrogen bonding between the EC2 and TMD 2, and introduced bulky amino acids to provide a repulsive force between the EC2 and the transmembrane bundle. In D196A K201A we ablated a salt bridge that appears to stabilise the closed conformation. Finally, we generated a mutant in which HCV binding is disrupted, this will act as control in subsequent functional assays (F186A).

CD81 is found in all vertebrates, Figure 3A displays the structure of CD81 colour coded for its amino acid conservation; the transmembrane domains and hinge regions of the EC2 display high conservation, whilst the apex of the EC2 exhibits increased diversity. This would suggest that the outward-facing apex is under positive selection to drive new interactions and/or to escape pathogen binding [51], whilst the lower region of the protein experiences negative selection to maintain residues that are essential for basic protein function. If conformational switching is an important feature of CD81 we may expect high conservation at the residues that regulate this process. Figure 3B is a phylogenetic tree constructed from representative vertebrate CD81 protein sequences and annotated to show the degree of conservation observed for the set of mutated residues described above. The proposed conformation-switching residues and cholesterol binding sites are all conserved, suggesting functional importance. Notably, the residues at 116 & 117 and 196 & 201 maintain the potential for salt bridge formation in 15/15 and 13/15 of the representative sequences; salt bridges are often observed stabilising conformational intermediates of a protein. Residue 186 is presented at the apex of CD81 (Fig. 2) and is critical for HCV binding; like much of the EC2, this position exhibits low conservation, consistent with the CD81-dependent species specificity of HCV infection.

Protein validation. In the next phase of our investigation we used lentiviral vectors to express our panel of CD81 mutants in Huh-7 cells that had been gene edited by CRISPR/Cas9 to ablate endogenous CD81 expression [36]. Huh-7 cells are highly permissive to lentiviral vectors allowing robust exoge-

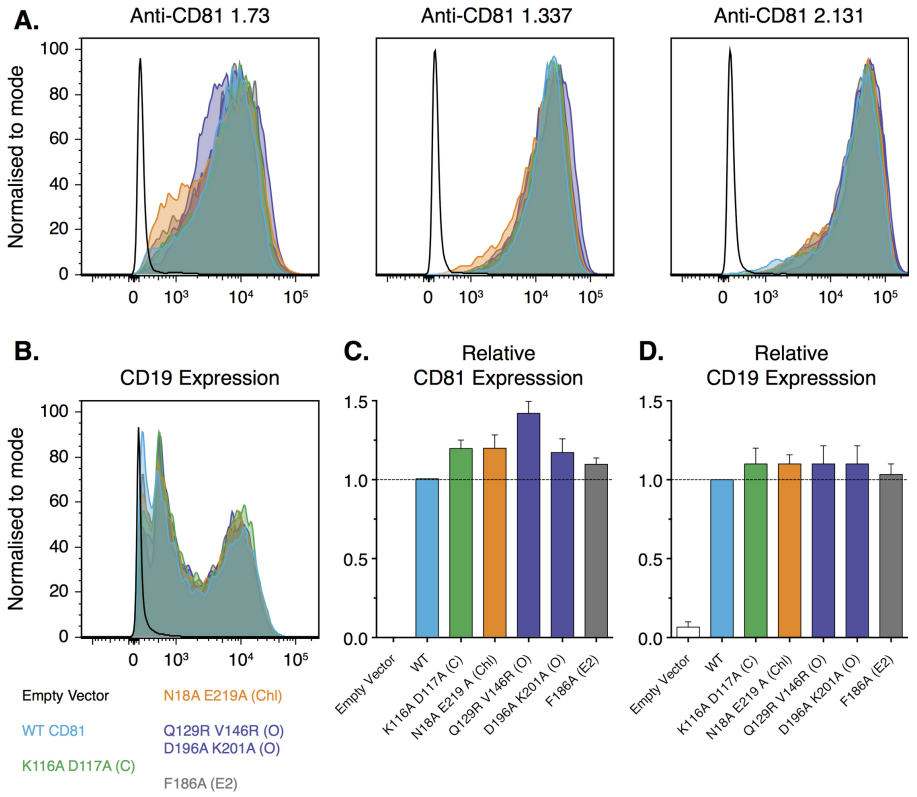

Fig. 4. CD81 mutants are properly folded and expressed The panel of CD81 variants were expressed in Huh-7 CD81 KO cells by lentiviral transduction. Variants are colour-coded, as indicated in the legend. **A.** Representative histograms displaying cell surface expression of CD81 variants as assessed by flow cytometry, using three distinct mAbs that recognise the EC2 of CD81. **B.** Representative histograms of exogenous cell surface CD19 expression in Huh-7 CD81 KO cells transduced with CD81 variants or control vector. Quantification of cell surface CD81 (C.) or CD19 (D.), data is expressed relative to WT, across three independent experiments; error bars indicate standard error of the mean.

nous gene expression. We first assessed cell surface expression of our mutants using a range of monoclonal antibodies (mAbs) that target diverse antigenic sites on the EC2 and are sensitive to proper protein folding [34,36]; mAb binding was measured by flow cytometry (Fig. 4A). As expected, the unmodified Huh-7 CD81 KO cells exhibited no antibody binding, whereas cells transduced with WT or mutant CD81 reacted to each of the anti-CD81 mAbs. No difference in mAb binding was observed between the mutants (Fig. 4C). To further validate the mutants we examined transduced cells by confocal microscopy (S1A Fig.). Anti-CD81 mAb 2.131 exhibited heterogeneous distribution across the cell surface with intense staining around the cell periphery; each of the mutants displayed a similar pattern and intensity of staining. These data indicate that the panel of mutants are equally well expressed at the cell surface and exhibit normal antigenicity. This also suggest that the mAbs cannot discriminate between the open and closed conformation of CD81, however, this is not necessarily surprising as the mAbs recognise outward-facing epitopes on the EC2 that are likely to be equally accessible in either conformation [34].

As described in the introduction, CD81 exerts its functions through interactions with various partner proteins. For instance, it facilitates B-cell receptor signalling by chaperoning CD19 through the secretory pathway and determining its cell surface distribution [10–12]. To provide an assay of basic CD81 function, we recapitulated CD81-dependent trafficking of CD19 in Huh-7 cells. Supplementary Figure 1B displays exogenous CD19 expression in Huh-7 cells +/- CD81, as assessed by fluorescence microscopy; no cell surface CD19 is detectable in Huh-7 CD81 KO cells, despite equivalent total CD19 expression (S. Fig. 1C). Figure 4B and D display CD81-dependent cell surface expression of CD19 in Huh-7 cells. Each of the mutants maintains their ability to chaperone CD19 to the plasma membrane; this is a further demonstration that the targeted mutations do not perturb CD81 trafficking or basic protein function.

HCV receptor activity. Having validated our CD81 variants we next set out to assess their function as receptors for HCV. We achieved this using a range of in vitro models of HCV entry and replication. First we used soluble E2 glycoprotein (sE2); this is the least authentic tool available to study HCV entry: E2 is presented without its partner protein, E1, and not in the context of a virion. Nonetheless, it is the only tool available to directly assess E2-CD81 interactions at the cell surface and therefore provides valuable information.

sE2 binding can be conferred to CHO cells by introduction of HCV receptors (CD81 or SR-B1) [52]. Therefore, we transduced CHO cells with our panel of variants and assessed binding of sE2 from the prototypical J6 and H77 strains. Figure 5A displays flow cytometry histograms of anti-CD81 mAb and sE2 binding; for clarity, representative plots are shown from CHO cells expressing WT CD81, the D196A K201A open mutant and the F186A E2 binding mutant. Figure 5B displays quantification for all conditions. Anti-CD81 binding was equivalent across all mutants, indicating proper cell surface expression (Fig. 5B). In agreement with other reports [4,42] the absolute level of CD81 binding was greater for H77 sE2 than for J6 (compare WT CD81 plots in Fig. 5A). Nonetheless, consistent differences between the CD81 mutants emerged (Fig. 5C & D).

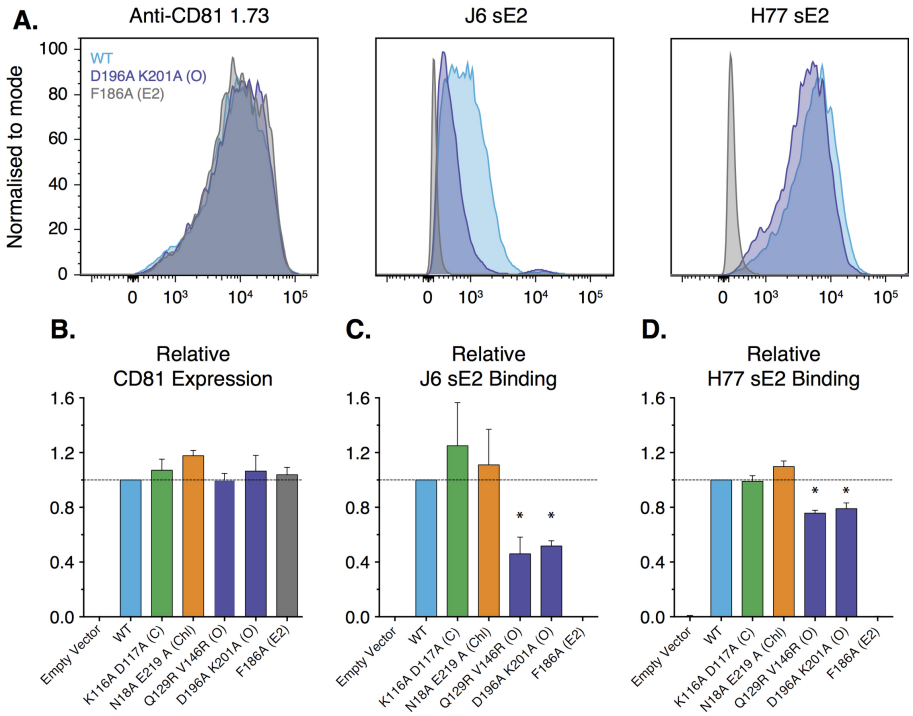

Fig. 5. Open CD81 mutants exhibit reduced binding to HCV E2 glycoprotein CHO cells were transduced to express CD81 variants and then assessed for their ability to bind sE2 by flow cytometry. **A.** Histograms displaying binding of anti-CD81, J6 sE2 and H77 sE2 to CHO cells expressing WT, D196A K201A (open) and F186A (E2) CD81; these examples are representative of the data acquired for the range of CD81 variants. **B.,C. and D.** Quantification of binding, expressed relative to WT CD81. Data compiled from three independent experiments, error bars indicate standard error of the mean. Asterisks indicate significant difference from WT: unpaired T-test, Graphpad Prism.

As expected, the E2 binding mutant (F186A) gave no signal, whereas the WT, closed (K116A D117A) and cholesterol-binding (N18A E219A) variants exhibited good sE2 binding. Both of the open mutants displayed significantly reduced sE2 binding; this was most apparent for the J6 strain. This finding is broadly consistent with the notion that the open conformation of CD81 is a poor receptor for HCV.

Whilst the sE2 binding assay provides a window on HCV-CD81 interactions, it is an inauthentic approach. Our subsequent experiments, therefore, sought to measure CD81 receptor activity in increasingly relevant systems.

In the HCV pseudoparticle (HCVpp) system, biologically active HCV E1E2 complexes are presented on the surface of lentivirus-based reporter virions [53,54]. This provides two major advantages: it allows the processes of HCV entry to be studied in isolation and is a robust platform for assessing diverse strains of HCV. Therefore we challenged Huh-7 cells, expressing the CD81 variants, with HCVpp bearing the glycoproteins of 8 strains of HCV from 5 different subtypes (1a, 2a, 2b, 4 and 5). Figure 6 displays HCVpp infections with three representative viruses and combined data for all 8 strains; example raw data from one experiment is shown in Supplementary Figure 2. Equivalent CD81 expression was verified by flow cytometry (data not shown).

The CD81 variants displayed consistent phenotypes across the diverse HCVpp strains. Much like the E2 binding mutant (F186A), the open mutants exhibited poor receptor activity; these data correlate with the observations in the sE2 assay (Fig. 5). Notably, in the context of the HCVpp assay the cholesterol-binding mutant displayed reduced receptor activity, to a similar degree as the open variants. Strikingly, the closed mutant was a better receptor, with HCVpp infection increasing by 50% (Fig. 6B).

As a final test of HCV receptor activity we turned to the HCV cell culture model (HCVcc); this generates fully infectious HCV and is considered to be the most authentic of the available in vitro systems [35,55]. Much like the HCVpp system, the open and cholesterol mutants display reduced ability to support HCVcc infection (Fig. 7). However, in this context the closed mutant conferred only a very modest ($\tilde{1}0\%$) enhancement in infection; whilst this reaches statistical significance, it is unclear whether it is biologically relevant. Direct comparison of the data acquired using the J6 HCVpp and J6/JFH HCVcc indicates excellent agreement (R^2= 0.96, S3 Fig.); this further demonstrates that HCVpp are a good model for HCV entry [56].

These models of HCV entry and infection provide data that are consistent with our original hypothesis: CD81 variants that are predicted to adopt an open conformation are poor receptors for HCV, whereas the closed variants retain normal (or potentially enhanced) receptor activity. The cholesterol-binding mutant also exhibits reduced ability to support HCV infection; this is broadly consistent with cholesterol binding being important for CD81 function and a potential regulator of conformational switching. However, these experiments do not directly explore the structural behaviour of our CD81 variants.

Conformational dynamics. Whilst there is currently no assay to directly assess CD81 conformation, we explored structural fluctuations in CD81 using molecular dynamics simulations. We ran two 1µs simulations for each mutant using a modelled lipid bilayer without cholesterol. Supplementary Figure 4 illustrates CD81, in a closed conformation, surrounded by a model bilayer. Figure 8 summarises our findings. Note that testing different parameters with multiple simulations for each mutant is not feasible due to the com-

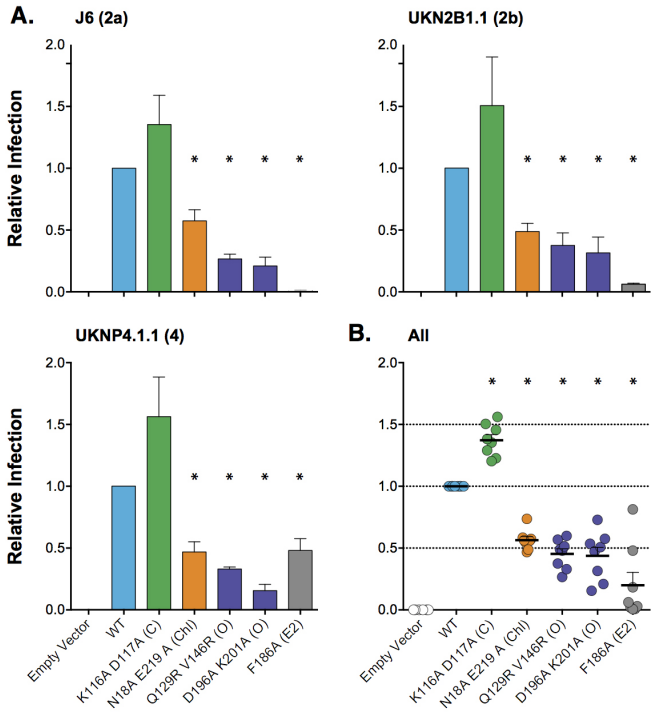

Fig. 6. CD81 open and cholesterol binding mutants are poor receptors for HCV entry Huh-7 CD81 KO cells were transduced to express CD81 variants and then challenged with diverse HCVpp. **A.** Representative plots for three strains of HCVpp; data is taken from three independent experiments and is expressed relative to signal in Huh-7 cells transduced with WT CD81. **B.** Compiled mean data (as in A.) from 8 strains of HCVpp. Error bars indicate standard error of the mean. Asterisks indicate significant difference from WT: unpaired T-test, Graphpad Prism.

putationally expensive nature of MD.

Consistent with Zimmerman et. al. we observed conformational switching of CD81; this was most apparent in simulation A of the N18A E219A mutant. Supplementary video 1 displays WT simulation A, in which the EC2 remains closed, whereas supplementary video 2 displays conformational switching in N18A E219A simulation A. We extracted a summary statistic from each simulation by measuring the angle of helix A of the EC2 relative to the vertical position of TMD 4. Figure 8A illustrates the time-dependent angular rotation of helix A observed during the simulations shown in the supplementary videos, Figure 8B plots this angle over time.

By performing the same analysis across each simulation we can assess the propensity of each mutant to undergo conformational switching. Figure 8C displays summaries for each 1µs simulation with individual data points representing the angle of helix A every 100ns. Snapshots provide representative images of helix A for each mutant. WT simulation A exhibited the least variation from the closed conformation (mean angle -0.672°) and was chosen as a reference for statistical analysis. Both simulations of the open mutants (Q129R V146R and D196A K201A) exhibit significantly larger angles than the WT reference, indicative of conformational switching. The closed mutant (K116A D117A) displayed no significant difference from the WT reference; this is to be expected, as this mutation is unlikely to perturb the closed conformation. As discussed above, one simulation for N18A E219A exhibited switching (Fig. 8A), however, the other simulation did not. That said, this experiment lacks cholesterol and, therefore, does not fully explore the potential phenotype of N18A E219A. Simulation B of WT CD81 exhibited statistically significant opening, however, this was largely driven by a single fluctuating data point.

In summary, our MD simulations are consistent with the observations of Zimmerman et. al. and suggest that our mutants are behaving broadly as designed. In particular the two open mutants displayed evidence of conformational switching in both duplicate simulations, whereas the closed mutant remained stable; these data are in line with our expectations and correlate very well with our in vitro experiments. The N18A E219A mutant also exhibited switching, albeit in the absence of cholesterol. One final consideration when interpreting these data is that the experiment simulates CD81 movement for just one millionth of a second (1µs), therefore, it cannot be assumed that these conformational switching events have reached their full extent; given longer simulations further opening of the EC2 may be possible.

In conclusion, this investigation uses a combination of structure-led mutagenesis, biological validation, functional characterisation and computational biology to yield consistent and coherent observations. This work provides evidence that CD81 conformational switching is a functionally relevant process.

Discussion

Like many tetraspanins, CD81 is a multifunctional protein that contributes to a variety of physiological and pathological processes [5,6]. The CD81 crystal structure, by Zimmerman et. al., provided a new perspective on tetraspanin biology [25] and proposed two novel features that may have relevance for protein function: i) CD81 is able to bind cholesterol in a cavity formed by its transmembrane domains and ii) the EC2 of CD81 undergoes conformational switching between a compact 'closed' form to an extended 'open' configuration. However, this original work did not fully explore the functional relevance of these observations. In this study, we investigated these structural features in the context of a well-characterised biological function: CD81's ability to mediate HCV attachment and entry. The importance of our work is two-fold; it provides further evidence for the conformational change put forward by Zimmerman et. al., and also suggests that this molecular switch alters CD81's ability to support HCV infection.

Our original hypothesis, that HCV entry favours the closed conformation of CD81, is supported by our experimental data; this is most apparent when comparing the closed and open variants. The closed mutant (K116A D117A) retains normal sE2 binding (Fig. 5) and is able to support robust HCV entry and infection (Fig. 6 & 7). Moreover, this variant conferred increased entry in the HCVpp system; whilst this was not completely supported by our HCVcc data, it may suggest enhanced receptor activity for the closed mutant. In contrast, both open mutants (Q129R V146R &

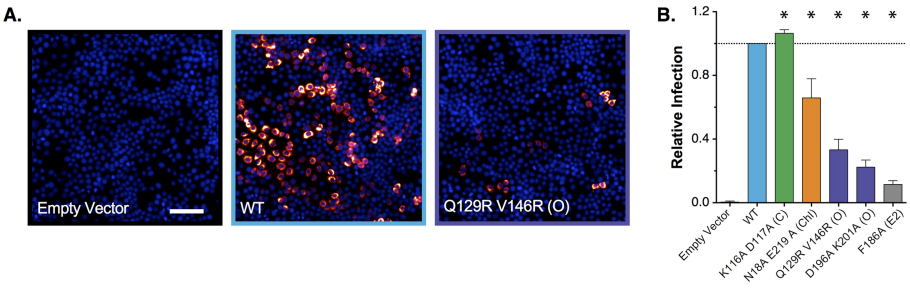

Fig. 7. CD81 open and cholesterol binding mutants are poor receptors for HCV infection Huh-7 CD81 KO cells were transduced to express CD81 variants and then challenged with J6/JFH HCVcc. **A.** Representative micrographs of HCVcc infection in transduced cells; DAPI nuclei shown in blue, viral antigen NS5A displayed in orange, scale bar = 100µm. **B.** Quantification of infection, compiled from four independent experiments, data is expressed relative to infection in cells expressing WT CD81. Error bars indicate standard error of the mean. Asterisks indicate significant difference from WT: unpaired T-test, Graphpad Prism.

D196R K201R) exhibited impaired sE2 binding and were very poor receptors for HCV entry and infection. Notably, these open variants produced indistinguishable results in our functional assays; this suggests they are phenotypically identical, as we would expect. A shortcoming of our study is the lack of a direct assay of CD81 conformation; whilst this may be achievable through crystallisation or single molecule FRET, we deemed this to be beyond the scope of this initial study. Nonetheless, we used MD simulations to explore the structural flexibility of our CD81 variants. Here, the variants behaved as expected, with the open mutants exhibiting a propensity for conformational switching; these data were in excellent agreement with our functional assays. In summary, starting with the original notion of CD81 conformational switching, we were able to design targeted mutations that yielded predictable phenotypes in both in vitro and computational experiments; this provides good evidence for conformational switching as a functionally important event.

Zimmerman et al. proposed that cholesterol binding may regulate CD81 conformational switching via an allosteric mechanism. Furthermore, there is a long-standing precedent in the literature for cholesterol being important for both tetraspanin function and HCV entry [26,49,50]. Therefore our study also included a CD81 variant in which the cholesterol binding residues had been mutated (N18A E219A). It may be expected that by preventing cholesterol binding we would increase the propensity for conformational switching; consistent with this, the cholesterol-binding mutant exhibited reduced receptor activity in the HCVpp and HCVcc system, in line with the open mutants. However, this variant was partially distinct from the open mutants, in particular it displayed normal sE2 binding, suggesting that CD81-E2 interactions are maintained. This makes interpretation of our results less straightforward and indicates that cholesterol binding and/or conformational switching may influence aspects of CD81 receptor function that are distinct from E2 binding. MD experiments clearly demonstrate conformational switching of the cholesterol-binding mutant in one simulation but not the repeat; this inconsistency and the fact that we chose to omit cholesterol from the MD simulations makes it difficult to draw unambiguous interpretations of this experiment. In summary, our data are not inconsistent with cholesterol regulating CD81 conformational switching and, therefore, HCV entry. However, nuances in the data mean that we cannot completely reconcile these observations with those made using the closed and open mutants. Fully understanding how cholesterol dictates CD81 receptor function will require further investigation.

Our work is consistent with other reports on CD81 receptor function. In a recent report, Banse et. al. swapped the human CD81 EC2 in to various CD81 orthologs and paralogs (e.g. zebrafish CD81 and CD9) to demonstrate that some determinants of HCV receptor activity lie outside of the EC2 [4]. Our work offers a potential explanation for these observations: whereby presentation of the human CD81 in a foreign context alters or prevents conformational switching and, therefore, reduces receptor function. In addition, the Banse et. al. study and an older report by Bertaux et. al. suggest transmembrane domain residues, including the cholesterol binding sites, also determine HCV receptor activity [57]; this further corroborates our findings.

It is also worth considering why a closed conformation of CD81 may be a better receptor. One potential explanation is biophysical; HCV binding occurs on the apex of the closed EC2, as indicated in Figure 1, therefore, it is possible that outward presentation of the EC2 favours receptor engagement. Furthermore, close physical proximity to the plasma membrane may also be beneficial. A recent report of the structure of HIV-1 gp120 in complex with its co-receptor CCR5 suggests that the principal role of CCR5 is to anchor the HIV fusion machinery in close apposition to the host membrane [58]; consequently the HIV fusion peptide is within striking distance upon activation. CD81 has been implicated in HCV fusion [59] and has a low profile at the cell surface, particularly in the closed conformation (S4 Fig.), therefore, it could perform an analogous anchoring function for the HCV glycoproteins. Under this mechanism, the open conformation of CD81 may generate an insurmountable gap between the viral and host membranes, therefore inhibiting fusion.

The HCV receptor function of CD81, much like its various physiological functions, is also likely to be dependent on its molecular partnerships. There is clear evidence for CD81 association with other HCV entry factors, most notably SR-B1, claudin-1 and EGFR [8,44,60,61]. Whether or not conformational switching is linked to these interactions is an important, and yet unanswered, question. Notably, SR-B1 funnels cholesterol from its lipoprotein ligands directly in to the plasma membrane [62,63]. Moreover, it is well established that HCV entry is enhanced by lipoproteins and that HCV particles themselves are lipoprotein-like being highly enriched for cholesterol [49]. Therefore, could localised delivery of cholesterol, from lipoproteins or HCV par-

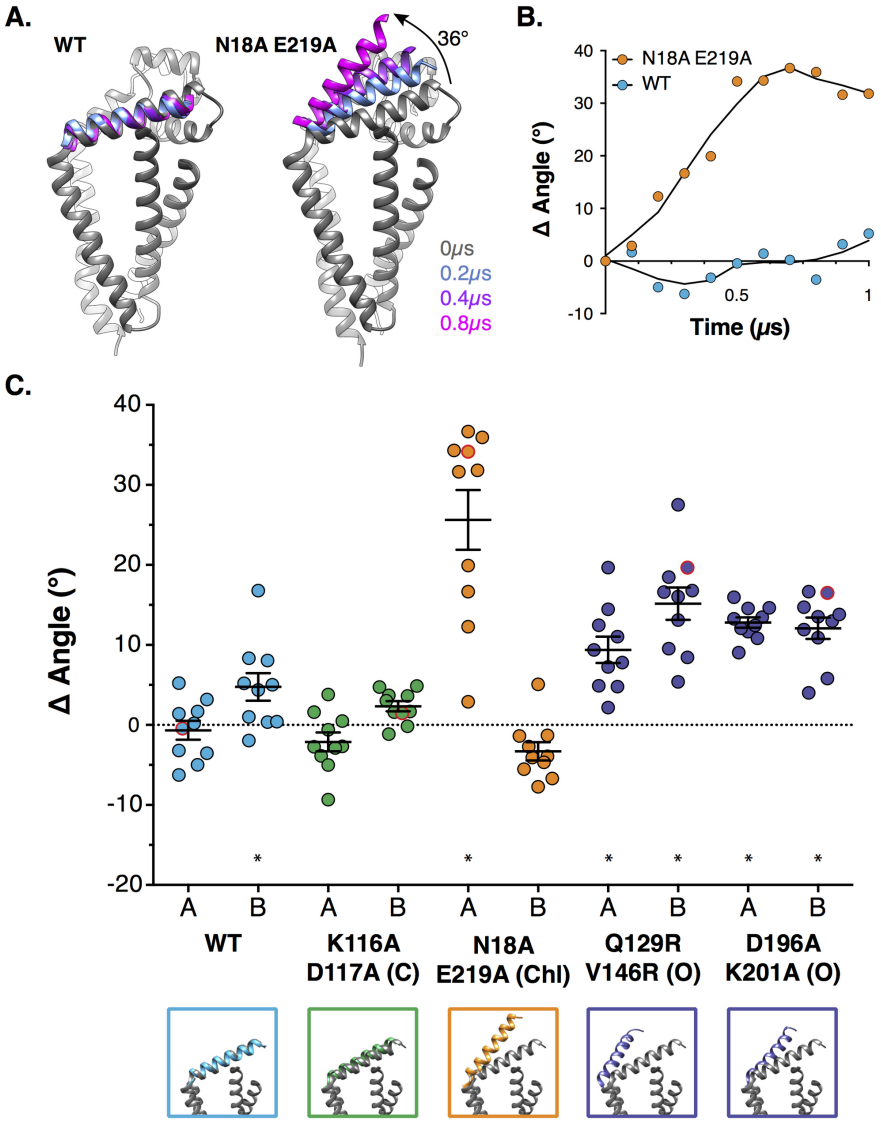

Fig. 8. CD81 mutants undergo conformational switching We performed duplicate 1μs MD simulations (labelled A and B) for WT CD81 and each of the mutants. **A.** Representative molecular models demonstrating conformational switching of CD81; the complete structure at 0μs is shown in grey, for clarity only helix A of the EC2 is shown for the subsequent time points, colour-coded as indicated. Images from the A simulation of WT and N18A E219A are shown, movies of these are provided in the supplementary materials. **B.** Quantification of the angular displacement of helix A for the simulations represented in A. The data was fitted with a smoothed line in Graphpad Prism. **C.** Quantification of the angular displacement of helix A for each simulation. The data points represent measurements made at 100ns intervals. Images are shown below each mutant with the backbone of CD81 at 0μs shown in grey and helix A from an illustrative frame shown in colour; the selected data points are outlined in red on the plot above. Error bars indicate standard error of the mean, asterisks indicate significant difference from the reference simulation (WT A): Mann-Whitney test, Graphpad Prism.

ticles via SR-B1, regulate CD81 function? Furthermore, the cholesterol transport function of SR-B1 has also been linked to CD81-dependent cellular invasion by *Plasmodium falciparum*; this process may also require conformational switching [46,47]. These questions, and their relevance to CD81's physiological functions, will be the focus of future research efforts.

Materials and methods

Cell culture. Huh-7 CD81 KO cells were a kind gift from Prof. Yoshiharu Matsuura (Osaka University, Japan) [36]. Huh-7.5 cells were acquired from Apath LLC. HEK293T and CHO-K1 cells were acquired from the American Type Culture Collection. All cells were grown at 37°C in DMEM supplemented with 10% foetal calf serum, 1% non-essential amino acids and 1% penicillin/ streptomycin.

Antibodies. Anti-NS5 and anti-CD81 mAbs were a kind gift from Prof. Jane McKeating (University of Oxford, UK). The anti-CD81 mAbs have been described in detail recently [34]. Anti-CD19 (sc-19650) was purchased from Santa Cruz Biotechnology. StrepMAb classic was purchased from IBA GmbH (Göttingen, Germany). All secondary antibodies purchased from Thermo Fisher Scientific (Waltham, MA, USA).

Lentiviral vectors. Commercially synthesised gene sequences encoding WT and mutant CD81 were inserted into lentiviral expression plasmids by restriction digest. CD19 was cloned into the same background through PCR amplification from human cDNA. These plasmids will be made freely available after publication: https://www.addgene.org/Joe_Grove/. To generate lentiviral vectors HEK293T cells were co-transfected with pCMV-dR8.91 packaging construct, pMD2.G VSV-G expression plasmid and one of each of the CD81 encoding plasmids. Supernatants containing viral vectors were collected at 48 and 72 hours. The transduction efficiency of vectors were titrated by flow cytometry to allow equivalent transduction and expression of CD81 variants.

HCV pseudoparticles. HCVpp were generated in a similar manner to the lentiviral expression vectors. HEK293T cells were cotransfected with pCMV-dR8.91 packaging construct, a luciferase reporter plasmid and an expression vector encoding the appropriate HCV glycoprotein. Supernatants containing HCVpp were collected at 48 and 72 hours. UKN4.1.1, 5.2.1, 2A1.2 and 2B1.1 E1E2 expression plasmids were kindly provided by Alex Tarr and Jonathan Ball (University of Nottingham, UK), all other E1E2 plasmids were generated in-house through PCR or commercial gene synthesis.

Cell culture proficient HCV. Plasmid encoding full-length J6/JFH genome was acquired from Apath LLC. HCVcc were generated as described previously. Briefly, in vitro transcribed full-length HCV RNA genomes were electroporated into Huh-7.5 cells. Supernatants containing infectious HCVcc were harvested every 2-4 hours during the day, from 3-7 days post electroporation. Harvests were then pooled, aliquoted and frozen to generate a standardised stock for infection assays.

Infections. Huh-7 cells were seeded at $1.5x10^4$ cells per well of a 96 well plate 24 hours prior to the experiment; to infect they were challenged with HCVpp/HCVcc supernatants (diluted 1/2 – 1/4 in DMEM 6% FCS). The infections were allowed to proceed for 72 hours before read out. For HCVpp, the samples were lysed and assayed using the SteadyGlo reagent kit and a GloMax luminometer (Promega, Maddison, WI, USA). To measure HCVcc replication, cells were fixed with 100% methanol and stained for viral NS5 protein. The proportion of infected cells was determined using the ImageJ Infection Counter plugin [64], these data were also verified by manually counting foci forming units.

Soluble E2 binding assay. J6 and H77 E2 ectodomains (residues 384-661) were PCR cloned into expression vectors, as previously described [52], with the resultant constructs including an upstream tissue plasminogen activator signal sequence (to direct efficient secretion) and a downstream strep-tag II (for detection and purification). Proteins were produced by transient transfection of HEK293T cells with the supernatants being harvested at 48 and 72 hours post infection. The sE2 binding assay was performed as previously described. A single-cell suspension of CHO +/- CD81 cells were preincubated in 'traffic stop' buffer, PBS + 1% bovine serum albumin (BSA) and 0.01% sodium azide; this depletes cellular ATP pools, consequently preventing receptor internalisation. All subsequent steps are performed in traffic stop buffer. Cells (100µl at $1\text{-}3x10^6$/ml) were then mixed with an equal volume of sE2 supernatant and incubated for 1 hour at 37°C. Bound sE2 was then detected using 3µg/ml StrepMab classic followed by an anti-mouse Alexa Fluor 647 secondary, 1 hour incubation each at room temperature. Finally, cells were fixed in 1% formaldehyde. Fluorescence signals were measured by flow cytometry.

Flow cytometry. To measure cell surface expression of CD81 or CD19, single-cell suspensions of Huh-7/CHO cells were fixed in 1% formaldehyde and then blocked in PBS + 1% BSA. All subsequent steps are performed in blocking buffer. Cells (100µl at $1\text{-}3x10^6$/ml) were then serially incubated with anti-receptor antibodies followed by anti-mouse Alexa Fluor 647 secondary, 1 hour incubation each at room temperature. Fluorescence signals were measured on a LSR Fortessa (BD, Franklin Lakes, NJ, USA) and data was analysed using FlowJo (FlowJo LLC, Ashland, OR, USA). The lentiviral vectors, described above, also express GFP (from a separate promoter); therefore, this GFP signal was used as an independent measure of transduction to identify positive cells during analysis.

Microscopy. One day prior to study, Huh-7 cells +/- CD81 and/or CD19 were seeded into standard 24 well plates at $1.2x10^4$ cells/well. Cells were then fixed (in situ) in 2% formaldehyde, blocked and stained, as described for flow cytometry, with the inclusion of a 10 minute DAPI counterstain at the end of the procedure. Samples were imaged on a Nikon Ti inverted microscope, through a 40X extra-long working distance objective, using a C2 confocal scan head with 405nm and 635nm laser illumination (Nikon Instruments, Tokyo, Japan). Multiple Z-stacks were acquired for each sample. Data was processed for display using FIJI/ImageJ [65,66].

Western Blot. One day prior to study, Huh-7 cells +/- CD81 and/or CD19 were seeded into standard 24 well plates at $4x10^4$ cells/well. Cells were then lysed using a buffer containing 20mM Tris-HCl, 135mM NaCl, 1% Triton-X 100 and 10% glycerol. The samples were then run on a TruPage 4-12% gel under non-reducing conditions and transferred on to nitrocellulose membrane. The blots were blocked in PBS + 2% milk solution + 0.1% Tween-20 and then probed by serial incubation with anti-receptor antibodies and goat anti-mouse secondary conjugated to horseradish peroxidase. Chemiluminescence signal was then measured in a Chemidoc MP (Bio Rad, Hercules, CA, USA).

Molecular dynamics simulations. We started with a molecular model of full-length CD81 in a closed conformation; this is based on the crystal structure (5TCX), as previously described, and was generously provided by Prof. Ron O. Dror and Dr. Brendan Kelly. All substitutions were introduced using Modeller software and AutoSub.py script available at https://github.com/williamdlees/AmberUtils. Protonation states were determined in MolProbity [67]. Models were then inserted into simulated palmitoyl-oleoyl-phosphatidylcholine (POPC) bilayers using CHARMM-GUI [67,68]. Note that, Zimmerman et. al. reported that conformational switching was occurred more often in the absence of cholesterol, therefore, to increase the likelihood of observing switching we omitted cholesterol from the model membrane. For MD simulations, each variant model was put through the same pipeline. First, the models were solvated in a rectangular box using TIP3 water molecules and 0.15 M of NaCl. The volume of the box was 5.5×10^5 Å^3 with the total of 6×10^4 atoms including around 148 lipid molecules. The CHARMM

36 force field was used for the simulations on GPUs using the CUDA version of PMEMD in Amber 16 [69–71]. Following minimisation and equilibration steps, 1µs production runs were simulated under constant pressure using the Monte Carlo barostat, semi-isotropic pressure coupling and constant temperature via the Langevin thermostat at 310 K. For duplicate simulations, the output from the equilibration stage was reassigned velocities, allowing a decorrelated independent simulation.

Sequence conservation analysis. Vertebrate CD81 encoding gene sequences were pulled from the NCBI database. Multiple sequence alignment and phylogenetic tree construction (using representative gene sequences) was performed using CLC sequence viewer (Qiagen, Hilden, Germany).

Molecular modeling. Molecular graphics and analyses performed with UCSF Chimera, developed by the Resource for Biocomputing, Visualization, and Informatics at the University of California, San Francisco, with support from NIH P41-GM103311 [72].

ACKNOWLEDGEMENTS
We are grateful to Jane McKeating for reagents and advise. Thank you to Greg Towers and Mphatso Kalemera for scientific criticism. Also, thank you to Nicole Finardi for her efforts on the project.

References

1. Pileri P, Uematsu Y, Campagnoli S, Galli G, Falugi F, Petracca R, et al. Binding of hepatitis C virus to CD81. Science. 1998;282: 938–941.

2. Kinchen VJ, Zahid MN, Flyak AI, Soliman MG, Learn GH, Wang S, et al. Broadly Neutralizing Antibody Mediated Clearance of Human Hepatitis C Virus Infection. Cell Host Microbe. 2018;24: 717–730.e5.

3. Flyak AI, Ruiz S, Colbert MD, Luong T, Crowe JE Jr, Bailey JR, et al. HCV Broadly Neutralizing Antibodies Use a CDRH3 Disulfide Motif to Recognize an E2 Glycoprotein Site that Can Be Targeted for Vaccine Design. Cell Host Microbe. 2018;24: 703–716.e3.

4. Banse P, Moeller R, Bruening J, Lasswitz L, Kahl S, Khan AG, et al. CD81 Receptor Regions outside the Large Extracellular Loop Determine Hepatitis C Virus Entry into Hepatoma Cells. Viruses. 2018;10. doi:10.3390/v10040207

5. Charrin S, Jouannet S, Boucheix C, Rubinstein E. Tetraspanins at a glance. J Cell Sci. 2014;127: 3641–3648.

6. Charrin S, le Naour F, Silvie O, Milhiet P-E, Boucheix C, Rubinstein E. Lateral organization of membrane proteins: tetraspanins spin their web. Biochem J. 2009;420: 133–154.

7. Gerold G, Meissner F, Bruening J, Welsch K, Perin PM, Baumert TF, et al. Quantitative Proteomics Identifies Serum Response Factor Binding Protein 1 as a Host Factor for Hepatitis C Virus Entry. Cell Rep. 2015;12: 864–878.

8. Bruening J, Lasswitz L, Banse P, Kahl S, Marinach C, Vondran FW, et al. Hepatitis C virus enters liver cells using the CD81 receptor complex proteins calpain-5 and CBLB. PLoS Pathog. 2018;14: e1007111.

9. van Zelm MC, Smet J, Adams B, Mascart F, Schandené L, Janssen F, et al. CD81 gene defect in humans disrupts CD19 complex formation and leads to antibody deficiency. J Clin Invest. 2010;120: 1265–1274.

10. Cherukuri A, Shoham T, Sohn HW, Levy S, Brooks S, Carter R, et al. The tetraspanin CD81 is necessary for partitioning of coligated CD19/CD21-B cell antigen receptor complexes into signaling-active lipid rafts. J Immunol. 2004;172: 370–380.

11. Shoham T, Rajapaksa R, Boucheix C, Rubinstein E, Poe JC, Tedder TF, et al. The tetraspanin CD81 regulates the expression of CD19 during B cell development in a postendoplasmic reticulum compartment. J Immunol. 2003;171: 4062–4072.

12. Mattila PK, Feest C, Depoil D, Treanor B, Montaner B, Otipoby KL, et al. The actin and tetraspanin networks organize receptor nanoclusters to regulate B cell receptor-mediated signaling. Immunity. 2013;38: 461–474.

13. Rocha-Perugini V, Zamai M, González-Granado JM, Barreiro O, Tejera E, Yañez-Mó M, et al. CD81 controls sustained T cell activation signaling and defines the maturation stages of cognate immunological synapses. Mol Cell Biol. 2013;33: 3644–3658.

14. Brimacombe CL, Wilson GK, Hübscher SG, McKeating JA, Farquhar MJ. A role for CD81 and hepatitis C virus in hepatoma mobility. Viruses. 2014;6: 1454–1472.

15. Diao J, Pantua H, Ngu H, Komuves L, Diehl L, Schaefer G, et al. Hepatitis C virus induces epidermal growth factor receptor activation via CD81 binding for viral internalization and entry. J Virol. 2012;86: 10935–10949.

16. Rubinstein E, Ziyyat A, Prenant M, Wrobel E, Wolf J-P, Levy S, et al. Reduced fertility of female mice lacking CD81. Dev Biol. 2006;290: 351–358.

17. Ohnami N, Nakamura A, Miyado M, Sato M, Kawano N, Yoshida K, et al. CD81 and CD9 work independently as extracellular components upon fusion of sperm and oocyte. Biol Open. 2012;1: 640–647.

18. Jin Y, Takeda Y, Kondo Y, Tripathi LP, Kang S, Takeshita H, et al. Double deletion of tetraspanins CD9 and CD81 in mice leads to a syndrome resembling accelerated aging. Sci Rep. 2018;8: 5145.

19. Nydegger S, Khurana S, Krementsov DN, Foti M, Thali M. Mapping of tetraspanin-enriched microdomains that can function as gateways for HIV-1. J Cell Biol. 2006;173: 795–807.

20. He J, Sun E, Bujny MV, Kim D, Davidson MW, Zhuang X. Dual Function of CD81 in Influenza Virus Uncoating and Budding. PLoS Pathog. 2013;9: e1003701.

21. Shaw ML, Stone KL, Colangelo CM, Gulcicek EE, Palese P. Cellular proteins in influenza virus particles. PLoS Pathog. 2008;4: e1000085.

22. Grove J. Super-resolution microscopy: a virus' eye view of the cell. Viruses. 2014;6: 1365–1378.

23. Rocha-Perugini V, Suárez H, Álvarez S, López-Martín S, Lenzi GM, Vences-Catalán F, et al. CD81 association with SAMHD1 enhances HIV-1 reverse transcription by increasing dNTP levels. Nat Microbiol. 2017;2: 1513–1522.

24. Silvie O, Rubinstein E, Franetich J-F, Prenant M, Belnoue E, Rénia L, et al. Hepatocyte CD81 is required for Plasmodium falciparum and Plasmodium yoelii sporozoite infectivity. Nat Med. 2003;9: 93–96.

25. Zimmerman B, Kelly B, McMillan BJ, Seegar TCM, Dror RO, Kruse AC, et al. Crystal Structure of a Full-Length Human Tetraspanin Reveals a Cholesterol-Binding Pocket. Cell. 2016;167: 1041–1051.e11.

26. Charrin S, Manié S, Thiele C, Billard M, Gerlier D, Boucheix C, et al. A physical and functional link between cholesterol and tetraspanins. Eur J Immunol. 2003;33: 2479–2489.

27. Silvie O. Cholesterol contributes to the organization of tetraspanin-enriched microdomains and to CD81-dependent infection by malaria sporozoites. J Cell Sci. 2006;119: 1992–2002.

28. Drummer HE, Boo I, Maerz AL, Poumbourios P. A conserved Gly436-Trp-Leu-Ala-Gly-Leu-Phe-Tyr motif in hepatitis C virus glycoprotein E2 is a determinant of CD81 binding and viral entry. J Virol. 2006;80: 7844–7853.

29. Drummer HE, Wilson KA, Poumbourios P. Determinants of CD81 dimerization and interaction with hepatitis C virus glycoprotein E2. Biochem Biophys Res Commun. 2005;328: 251–257.

30. Drummer HE, Wilson KA, Poumbourios P. Identification of the Hepatitis C Virus E2 Glycoprotein Binding Site on the Large Extracellular Loop of CD81. J Virol. 2002;76: 11143–11147.

31. Keck Z-Y, Saha A, Xia J, Wang Y, Lau P, Krey T, et al. Mapping a region of hepatitis C virus E2 that is responsible for escape from neutralizing antibodies and a core CD81-binding region that does not tolerate neutralization escape mutations. J Virol. 2011;85: 10451–10463.

32. Kong L, Giang E, Nieusma T, Kadam RU, Cogburn KE, Hua Y, et al. Hepatitis C virus E2 envelope glycoprotein core structure. Science. 2013;342: 1090–1094.

33. Higginbottom A, Quinn ER, -C. Kuo C, Flint M, Wilson LH, Bianchi E, et al. Identification of Amino Acid Residues in CD81 Critical for Interaction with Hepatitis C Virus Envelope Glycoprotein E2. J Virol. 2000;74: 3642–3649.

34. Grove J, Hu K, Farquhar MJ, Goodall M, Walker L, Jamshad M, et al. A new panel of epitope mapped monoclonal antibodies recognising the prototypical tetraspanin CD81. Wellcome Open Res. 2017;2: 82.

35. Lindenbach BD, Evans MJ, Syder AJ, Wölk B, Tellinghuisen TL, Liu CC, et al. Complete replication of hepatitis C virus in cell culture. Science. 2005;309: 623–626.

36. Yamamoto S, Fukuhara T, Ono C, Uemura K, Kawachi Y, Shiokawa M, et al. Lipoprotein Receptors Redundantly Participate in Entry of Hepatitis C Virus. PLoS Pathog. 2016;12: e1005610.

37. Flint M, von Hahn T, Zhang J, Farquhar M, Jones CT, Balfe P, et al. Diverse CD81 proteins support hepatitis C virus infection. J Virol. 2006;80: 11331–11342.

38. Fofana I, Xiao F, Thumann C, Turek M, Zona L, Tawar RG, et al. A novel monoclonal anti-CD81 antibody produced by genetic immunization efficiently inhibits Hepatitis C virus cell-cell transmission. PLoS One. 2013;8: e64221.

39. Koutsoudakis G, Herrmann E, Kallis S, Bartenschlager R, Pietschmann T. The level of CD81 cell surface expression is a key determinant for productive entry of hepatitis C virus into host cells. J Virol. 2007;81: 588–598.

40. Zhang J, Randall G, Higginbottom A, Monk P, Rice CM, McKeating JA. CD81 is required for hepatitis C virus glycoprotein-mediated viral infection. J Virol. 2004;78: 1448–1455.

41. Owsianka A, Tarr AW, Juttla VS, Lavillette D, Bartosch B, Cosset F-L, et al. Monoclonal antibody AP33 defines a broadly neutralizing epitope on the hepatitis C virus E2 envelope glycoprotein. J Virol. 2005;79: 11095–11104.

42. Sabo MC, Luca VC, Prentoe J, Hopcraft SE, Blight KJ, Yi M, et al. Neutralizing monoclonal antibodies against hepatitis C virus E2 protein bind discontinuous epitopes and inhibit infection at a postattachment step. J Virol. 2011;85: 7005–7019.

43. Giang E, Dorner M, Prentoe JC, Dreux M, Evans MJ, Bukh J, et al. Human broadly neutralizing antibodies to the envelope glycoprotein complex of hepatitis C virus. Proc Natl Acad Sci U S A. 2012;109: 6205–6210.

44. Harris HJ, Davis C, Mullins JGL, Hu K, Goodall M, Farquhar MJ, et al. Claudin association with CD81 defines hepatitis C virus entry. J Biol Chem. 2010;285: 21092–21102.

45. Ding Q, von Schaewen M, Ploss A. The impact of hepatitis C virus entry on viral tropism. Cell Host Microbe. 2014;16: 562–568.

46. Yalaoui S, Huby T, Franetich J-F, Gego A, Rametti A, Moreau M, et al. Scavenger receptor BI boosts hepatocyte permissiveness to Plasmodium infection. Cell Host Microbe. 2008;4: 283–292.

47. Rodrigues CD, Hannus M, Prudêncio M, Martin C, Gonçalves LA, Portugal S, et al. Host Scavenger Receptor SR-BI Plays a Dual Role in the Establishment of Malaria Parasite Liver Infection. Cell Host Microbe. 2008;4: 271–282.

48. Lupberger J, Felmlee DJ, Baumert TF. Cholesterol uptake and hepatitis C virus entry. J Hepatol. 2012;57: 215–217.

49. Felmlee D, Hafirassou M, Lefevre M, Baumert T, Schuster C. Hepatitis C Virus, Cholesterol and Lipoproteins — Impact for the Viral Life Cycle and Pathogenesis of Liver Disease. Viruses. 2013;5: 1292–1324.

50. Kapadia SB, Barth H, Baumert T, McKeating JA, Chisari FV. Initiation of hepatitis C virus infection is dependent on cholesterol and cooperativity between CD81 and scavenger receptor B type I. J Virol. 2007;81: 374–383.

51. Forni D, Cagliani R, Pontremoli C, Pozzoli U, Vertemara J, De Gioia L, et al. Evolutionary Analysis Provides Insight Into the Origin and Adaptation of HCV. Front Microbiol. 2018;9: 854.

52. Grove J, Nielsen S, Zhong J, Bassendine MF, Drummer HE, Balfe P, et al. Identification of a residue in hepatitis C virus E2 glycoprotein that determines scavenger receptor BI and CD81 receptor dependency and sensitivity to neutralizing antibodies. J Virol. 2008;82: 12020–12029.

53. Hsu M, Zhang J, Flint M, Logvinoff C, Cheng-Mayer C, Rice CM, et al. Hepatitis C virus glycoproteins mediate pH-dependent cell entry of pseudotyped retroviral particles. Proceedings of the National Academy of Sciences. 2003;100: 7271–7276.

54. Bartosch B, Dubuisson J, Cosset F-L. Infectious hepatitis C virus pseudoparticles containing functional E1-E2 envelope protein complexes. J Exp Med. 2003;197: 633–642.

55. Lindenbach BD, Meuleman P, Ploss A, Vanwolleghem T, Syder AJ, McKeating JA, et al. Cell culture-grown hepatitis C virus is infectious in vivo and can be recultured in vitro. Proc Natl Acad Sci U S A. 2006;103: 3805–3809.

56. Wasilewski LN, Ray SC, Bailey JR. Hepatitis C virus resistance to broadly neutralizing antibodies measured using replication-competent virus and pseudoparticles. J Gen Virol. 2016;97: 2883–2893.

57. Bertaux C, Dragic T. Different domains of CD81 mediate distinct stages of hepatitis C virus pseudoparticle entry. J Virol. 2006;80: 4940–4948.

58. Shaik MM, Peng H, Lu J, Rits-Volloch S, Xu C, Liao M, et al. Structural basis of coreceptor recognition by HIV-1 envelope spike. Nature. 2019;565: 318–323.

59. Sharma NR, Mateu G, Dreux M, Grakoui A, Cosset F-L, Melikyan GB. Hepatitis C virus is primed by CD81 protein for low pH-dependent fusion. J Biol Chem. 2011;286: 30361–30376.

60. Lupberger J, Zeisel MB, Xiao F, Thumann C, Fofana I, Zona L, et al. EGFR and EphA2 are host factors for hepatitis C virus entry and possible targets for antiviral therapy. Nat Med. 2011;17: 589–595.

61. Baktash Y, Madhav A, Coller KE, Randall G. Single Particle Imaging of Polarized Hepatoma Organoids upon Hepatitis C Virus Infection Reveals an Ordered and Sequential Entry Process. Cell Host Microbe. 2018;23: 382–394.e5.

62. Gillard BK, Randall Bassett G, Gotto AM, Rosales C, Pownall HJ. Scavenger receptor B1 (SR-B1) profoundly excludes high density lipoprotein (HDL) apolipoprotein AII as it nibbles HDL-cholesteryl ester. J Biol Chem. 2017;292: 8864–8873.

63. Neculai D, Schwake M, Ravichandran M, Zunke F, Collins RF, Peters J, et al. Structure of LIMP-2 provides functional insights with implications for SR-BI and CD36. Nature. 2013;504: 172–176.

64. Culley S, Towers GJ, Selwood DL, Henriques R, Grove J. Infection Counter: Automated Quantification of in Vitro Virus Replication by Fluorescence Microscopy. Viruses. 2016;8. doi:10.3390/v8070201

65. Schneider CA, Rasband WS, Eliceiri KW. NIH Image to ImageJ: 25 years of image analysis. Nat Methods. 2012;9: 671–675.

66. Schindelin J, Arganda-Carreras I, Frise E, Kaynig V, Longair M, Pietzsch T, et al. Fiji: an open-source platform for biological-image analysis. Nat Methods. 2012;9: 676–682.

67. Chen VB, Arendall WB 3rd, Headd JJ, Keedy DA, Immormino RM, Kapral GJ, et al. MolProbity: all-atom structure validation for macromolecular crystallography. Acta Crystallogr D Biol Crystallogr. 2010;66: 12–21.

68. Jo S, Kim T, Iyer VG, Im W. CHARMM-GUI: a web-based graphical user interface for CHARMM. J Comput Chem. 2008;29: 1859–1865.

69. Maier JA, Martinez C, Kasavajhala K, Wickstrom L, Hauser KE, Simmerling C. ff14SB: Improving the Accuracy of Protein Side Chain and Backbone Parameters from ff99SB. J Chem Theory Comput. 2015;11: 3696–3713.

70. Salomon-Ferrer R, Götz AW, Poole D, Le Grand S, Walker RC. Routine Microsecond Molecular Dynamics Simulations with AMBER on GPUs. 2. Explicit Solvent Particle Mesh Ewald. J Chem Theory Comput. 2013;9: 3878–3888.

71. Le Grand S, Götz AW, Walker RC. SPFP: Speed without compromise—A mixed precision model for GPU accelerated molecular dynamics simulations. Comput Phys Commun. 2013;184: 374–380.

72. Pettersen EF, Goddard TD, Huang CC, Couch GS, Greenblatt DM, Meng EC, et al. UCSF Chimera–a visualization system for exploratory research and analysis. J Comput Chem. 2004;25: 1605–1612.